Unified description of odd-mass In nuclei. III. Application to ^{119,121}In

K. Heyde
Institut de Physique Nucléaire (and IN2P3), Université Lyon I 43, Bd du 11 Novembre 1918, 69622 Villeurbanne Cedex, France and Institute for Nuclear Physics, Proeftuinstraat 86, B-9000 Gent, Belgium

M. Waroquier and P. Van Isacker
Institute for Nuclear Physics, Proeftuinstraat 86, B-9000 Gent, Belgium

(Received 7 February 1980)

We describe the odd-mass indium nuclei $A = 119$, 121 within the framework of the unified-model taking into account the coupling of single-hole and one-particle–two-hole proton configurations with quadrupole and octupole vibrations of the underlying core. Besides the energy spectra, spectroscopic factors for pickup and electromagnetic transition properties [branching ratios, $T_{1/2}(1/2_1^+)$; $\delta(3/2_1^- \rightarrow 1/2_1^-)$] are calculated and compared with experimental data, mainly for ^{119}In. The yrast structure of the vibrational multiplet states has also been studied in lowest order perturbation theory and in the unified-model description. These calculations are also approached from a deformed zero-order description giving the total potential energy surfaces of all odd-mass In nuclei. Extensive band-mixing calculations produce energy spectra for the $1/2^+$ rotational-like band and are used to calculate static moments and transition rates. The equivalence with the former, spherical description is pointed out.

[NUCLEAR STRUCTURE Unified-model calculations, ^{119}In and ^{121}In, level schemes, branching ratios $T_{1/2}(\frac{1}{2}_1^+)$, $\delta(\frac{3}{2}_1^- \rightarrow \frac{1}{2}_1^-)$; yrast structure of vibrational multiplet, deformed description; total potential energy surfaces; Coriolis band-mixing.]

I. INTRODUCTION

In a recent article,[1] hereafter referred to as I, we tried to construct a unified-model description of odd-mass In nuclei. The theory was subsequently applied to ^{115}In (I) and ^{117}In (Ref. 2; hereafter referred to as II). Here we would like to extend the unified-model description to the heavier odd-mass isotopes ^{119,121}In, as discussed in detail in Secs. III and IV. Only some of the relevant formulas will be given because a detailed discussion and derivation of the formulas was given in I. Within the scope of this paper, measured branching ratios for ^{119}In will be calculated and compared extensively, a feature that was not studied in our earlier papers (I and II). Moreover, the $E2/M1$ mixing ratio for the $J_i^\pi = \frac{3}{2}_1^-$ to $J_f^\pi = \frac{1}{2}_1^-$ transition is discussed in some detail as well as the yrast structure of positive parity states, starting from the $J^\pi = \frac{9}{2}^+$ ground state in ^{119}In (Sec. III). Finally, in Sec. IV, a comparison with calculations in a deformed basis will be given.

II. HAMILTONIAN AND PARAMETERS

The model Hamiltonian for describing single-hole (1h) as well as one-particle–two-hole (1p-2h) (seniority $v=1$, $v=3$) configurations can be written as

$$H = E_0 + \sum_\lambda b_\lambda^\dagger b_\lambda [\hbar\omega_\lambda + (2\lambda+1)/2] + \sum_a \epsilon_a N(C_\alpha^\dagger C_\alpha)$$
$$+ \sum_{\alpha,\beta,\lambda,\mu} (\pi/2\lambda+1)^{1/2} \xi_\lambda \hbar\omega_\lambda \langle\alpha | Y_{\lambda\mu} | \beta\rangle N(C_\alpha^\dagger C_\beta)$$
$$\times (b_{\lambda\mu} + (-1)^\mu b_{\lambda-\mu}^\dagger)$$
$$+ \tfrac{1}{4} \sum_{\alpha,\beta,\gamma,\delta} \langle\alpha\beta | V | \gamma\delta\rangle N(C_\alpha^\dagger C_\beta^\dagger C_\delta C_\gamma), \qquad (2.1)$$

in which E_0 denotes the total energy of the $J^\pi = 0^+$ ground state in doubly-even Sn nuclei. The normal product $N(\ldots)$, is defined with respect to this physical ground state $|\tilde{0}\rangle$. The core-coupling term takes into account the particle, hole, and particle-hole core coupling, whereas $\langle\alpha\beta | V | \gamma\delta\rangle$ takes into account the residual interaction within the 1p-2h configurations.

The wave function describing excitations in the odd-mass In isotopes consists of hole-core (Sn) coupled states[3]

$$|j_h^{-1}, \mathrm{Sn}(R); JM\rangle \equiv [\tilde{C}_h \otimes \Omega_R^\dagger(\mathrm{Sn})]_{JM} |\tilde{0}\rangle \qquad (2.2)$$

and particle-core (Cd) coupled states[4]

$$|j_p, \mathrm{Cd}(I,i); JM\rangle \equiv [C_p^\dagger \otimes \Omega_{I,i}^\dagger(\mathrm{Cd})]_{JM} |\tilde{0}\rangle, \qquad (2.3)$$

where the Cd eigenstates $\Omega_{I,i}^\dagger$ (Cd) have been obtained (see I) by diagonalizing the hole-core and hole-hole interaction explicitly. The final wave functions, after diagonalizing the total Hamiltonian (2.1), then result in

$$|J^\alpha M\rangle = \sum_{h,R} h^\alpha(hR;J)\,|j_h^{-1}, \mathrm{Sn}(R); JM\rangle + \sum_{p,I,i} p^\alpha(pIi;J)\,|j_p, \mathrm{Cd}(I,i); JM\rangle\,. \quad (2.4)$$

In the calculations carried out in this paper and discussed in detail in Secs. III and IV, three different kinds of parameters occur: single-particle and single-hole energies, coupling strengths, and the residual hole-hole interaction $\langle\alpha\beta|V|\gamma\delta\rangle$. The phonon energies $\hbar\omega_2$, $\hbar\omega_3$ are taken from the excitation energy for the $J_i^\pi = 2_1^+$ and 3_1^- levels. The relation

$$\xi_2\hbar\omega_2 = \left\langle r\frac{\partial V}{\partial r}\right\rangle \frac{4(5\pi)^{1/2}}{3ZeR_0^{\,2}} B(E2; 2_1^+ \rightarrow 0_1^+)^{1/2} \quad (2.5)$$

was used to determine the hole-core (Sn) and particle-core (Cd) coupling strengths ξ_2. Since only the $B(E2)$ values of ^{120,122}Sn are known,[5] we carry out the same procedure as that used in Eq. (4.10) of I to calculate the particle-core (Cd) macroscopic matrix element, using the $(\xi_2\hbar\omega_2)_{\mathrm{Sn}}$ values.

As a residual interaction, a δ-function force without spin exchange and with strength parameter as determined for ^{115}In (I) was used. Concerning the single-particle states, the $1g_{9/2}^{-1}$, $2p_{3/2}^{-1}$, $2p_{1/2}^{-1}$, and $1f_{5/2}^{-1}$ levels are considered; the energies of the latter three chosen such as to give good fits to the experimentally observed $J_i^\pi = \frac{3}{2}_1^-$, $\frac{1}{2}_1^-$, and $\frac{5}{2}_1^-$ levels. (For excitation energies see Refs. 6–8; for spectroscopic factors see Refs. 9 and 10.) The energy for configurations in which a proton has been excited through the $Z=50$ closed shell is determined from the Wapstra and Bos mass tables[11] to be $S_p(Z=51,N) - S_p(Z=50,N)$, yielding a value of 2.5 MeV (rounded-off values) in both ^{119}In and ^{121}In. The relative energies (relative to $1g_{7/2}$) for the particle states above $Z=50$ ($2d_{3/2}$, $3s_{1/2}$, and $1h_{11/2}$) have been taken from Reehal and Sorensen,[12] whereas $\epsilon_{2d_{5/2}} - \epsilon_{1g_{7/2}}$ was taken as a parameter to fix the relative position of the lowest $J^\pi = \frac{1}{2}^+$ and $\frac{3}{2}^+$ states. The single-particle (hole) energies for ^{119,121}In are summarized in Table I.

In the actual calculations, up to three-quadrupole phonon and two-octupole phonon vibrations are considered, whereas in ^{118,120}Cd, all levels up to $E_x = 2$ MeV are used. This energy cutoff rougly corresponds to a macroscopic calculation with up to three-quadrupole phonon and two-octupole phonon vibrations if a more phenomenological particle-core (Cd) calculation is performed. Unperturbed configurations [Eqs. (2.2) and (2.3)] up to $E_x = 8.0$ MeV are used to screen out truncation effects below $E_x \cong 2.5$ MeV in the final ^{119,121}In nuclei.

TABLE I. Single-particle (ϵ_{nlj}) and single-hole energies ($\tilde{\epsilon}_{nlj}$). Energies are relative with respect to the $1g_{7/2}$ level (particles) and to the $1g_{9/2}$ level (holes).

	$\tilde{\epsilon}_{2p1/2}$	$\tilde{\epsilon}_{2p3/2}$	$\tilde{\epsilon}_{1f5/2}$	$\epsilon_{2d5/2}$	$\epsilon_{2d3/2}$	$\epsilon_{3s1/2}$	$\epsilon_{1h11/2}$
^{119}In	0.60	1.20	1.90	1.0	2.60	2.95	2.10
^{121}In	0.60	1.20	1.90	1.0	2.60	2.95	2.10

III. RESULTS

A. Energy spectra of ^{119,121}In

In Figs. 1 and 2, the unified-model calculated energy spectra are compared with the experimental data.[6-8] One can clearly observe the good agreement for the single-hole states as well as for the $|1g_{9/2}^{-1}, \mathrm{Sn}(2_1^+); JM\rangle$ multiplet (levels with open triangle marked). The rotational-like sequence of positive-parity states ($J^\pi = \frac{1}{2}^+, \frac{3}{2}^+, \ldots$), which seems to be well established in ^{119}In, is very nicely reproduced and mainly results from the interplay between (i) single-particle excita-

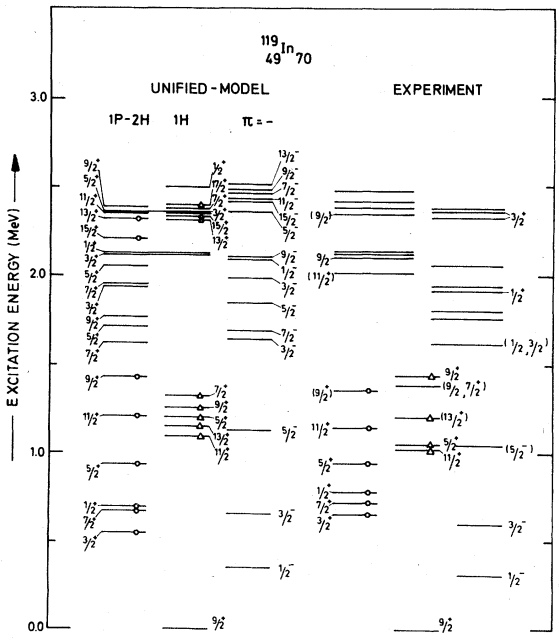

FIG. 1. The positive- and negative-parity levels of ^{119}In calculated in a unified-model description are compared with the experimental data. Levels marked with a small triangle have mainly a hole-core (Sn) character whereas the levels marked with a small circle are mainly particle-core (Cd) coupled stated. Levels with a line in both the 1p-2h and 1h column have strongly mixed character.

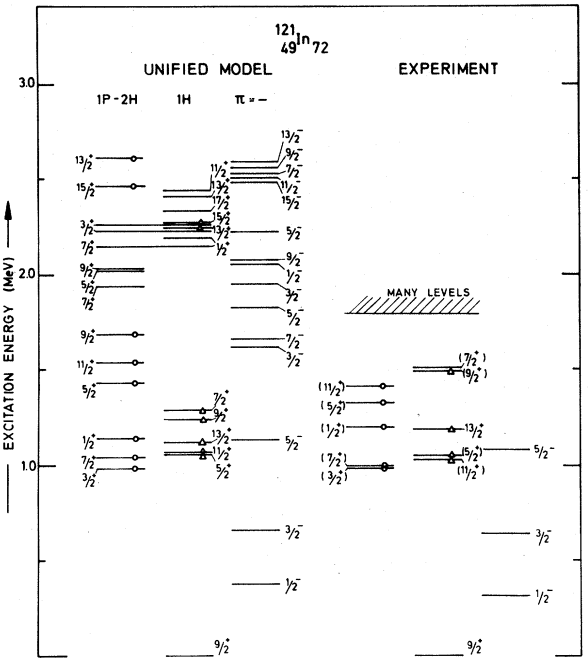

FIG. 2. Same as Fig. 1, but for ^{121}In.

tions through $Z=50$ for the corresponding J^π and (ii) large admixtures of $|2d_{5/2}, \mathrm{Cd}(2_1^+); JM\rangle$ and $|1g_{7/2}, \mathrm{Cd}(2_1^+); JM\rangle$ configurations. In ^{121}In, however, all spins are not determined,[6] although here again this particular rotational sequence seems to be observed.[13,14] A shift from the $J_i^\pi = \frac{1}{2}_1^+$ band head towards higher excitation energy becomes clear when going from ^{119}In to ^{121}In, a fact that can be related to the change in stiffness of the macroscopic Cd core [$E_x(2_1^+)$ is growing from 0.488 to 0.506 MeV for the variation ^{118,120}Cd; see also Sec. IV]. For ^{119}In, as was the case in ^{115}In, three states (with $J^\pi = \frac{9}{2}^+, \frac{7}{2}^+$ assignments) seem to occur near $E_x \cong 1.5$ MeV (only two such states result in the work of McDonald *et al.*[8]), which is also the case in the calculated spectrum. The theoretical $J_i^\pi = \frac{9}{2}_2^+$ level is the vibrational $|1g_{9/2}^{-1}, \mathrm{Sn}(2_1^+)\rangle$ multiplet configuration, whereas at $E_x(\text{theory}) \cong 1.43$ and 1.77 MeV, the $J_i^\pi = \frac{9}{2}_{3,4}^+$ levels occur, mainly built from the $|1g_{7/2}, \mathrm{Cd}(2_1^+)\rangle$ and $|2d_{5/2}, \mathrm{Cd}(2_1^+)\rangle$ configurations, respectively. In the theoretical spectrum, however, a $J_i^\pi = \frac{7}{2}_2^+$ level also occurs, which is built mainly from the the $|1g_{9/2}^{-1}, \mathrm{Sn}(2_1^+)\rangle$ configuration. The deexcitation pattern of this experimental $(\frac{9}{2}^+, \frac{7}{2}^+)$ level at 1.3885 MeV very well resembles the pattern resulting for the experimental $J^\pi = \frac{9}{2}^+$ level at 1.4365 MeV, the level which should correspond to the quadrupole vibrational multiplet (see also Table II). This argument can serve as a good explanation of the experimental situation in ^{119}In near $E_x \cong 1.5$ MeV.

Therefore, below $E_x \cong 1.5$ MeV, all levels in ^{119}In have a unique explanation in terms of the unified-model description although a small problem still remains with unique spin assignments for the three levels near $E_x \cong 1.5$ MeV.

In ^{121}In, unique spin and parity assignments are not available for all low-lying ($E_x \lesssim 1.5$ MeV) levels.[6] From the (p, α) experiments of Smits *et al.*[10] and the $(d, {}^3\mathrm{He})$ pickup reactions studies from Weifenbach,[9] the $J^\pi = \frac{13}{2}^+, \frac{9}{2}^+$ assignments could be made. Now, in further comparing the deexcitation pattern from the positive parity states with $0.95\ \mathrm{MeV} < E_x < 1.5$ MeV, with transitions in ^{119}In, suggestions for J^π can be made[13,14] (indicated between brackets on Fig. 2). Then the agreement with the unified-model description is again very good. Although model-dependent arguments were used in Refs. 13 and 14, we think that most levels of the vibrational multiplet as well as the $J^\pi = \frac{1}{2}^+, \frac{3}{2}^+, \frac{5}{2}^+, \frac{7}{2}^+$, and $\frac{11}{2}^+$ levels from the rotational band, have been observed.

As was pointed out already in I and will be discussed in Sec. IV, a description in terms of a rotational band built on top of the $\frac{1}{2}^+$ [431] Nilsson orbital, including Coriolis mixing with the other $N=4$ Nilsson orbitals, can serve as an alternative explanation for the positive-parity band sequence in ^{119,121}In.

B. Nuclear reaction and electromagnetic properties

1. Spectroscopic factors

The single-particle and single-hole components of the calculated wave functions can undergo a first test in the comparison of calculated and measured spectroscopic factors. Since only proton pickup reactions have been carried out,[9] we only give the theoretical spectroscopic factor for pickup as

$$S_{i,j}^{(\alpha)}(J) = \overline{h^\alpha(lj, 0_1^+; J)^2} \cdot \delta_{jJ} \,. \tag{3.1}$$

In Figs. 3(a) and 3(b) we compare (3.1) with the results of Weifenbach[9] for the wave functions calculated. The agreement for the lowest $J^\pi = \frac{9}{2}^+, \frac{1}{2}^-, \frac{3}{2}^-, \frac{5}{2}^-$ states is very good, although for the $E_x = 1.437$ $J^\pi = \frac{9}{2}^+$ level (supporting the discussion of Sec. III A), the theoretical value is too small. Above $E_x \cong 1.5$ MeV, only small fractions of $l=1$, $l=3$, and $l=4$ strength are calculated.

2. Branching ratios

In ^{119}In we have calculated many branching ratios in order to find out about other properties of the nuclear wave functions that have not been

TABLE II. Table of branching ratios as calculated with the unified-model wave functions. Both the total transition probabilities and the branching ratios are given for $g_R = Z/A$ and $g_R = 0$. Comparison is carried out with the experimental data of Scheideman *et al.* and of McDonald *et al.*

	$P_{tot}(s^{-1})$		Branching ratio			
$J_i^\pi \to J_f^\pi$	$g_R = Z/A$	$g_R = 0$	$g_R = Z/A$	$g_R = 0$	exp[a]	exp[b]
$*\frac{3^+}{2_1} \to \frac{3^-}{2_1}$	0.36×10^{8}		0.4		4.5	2
$\to \frac{1^-}{2_1}$	0.76×10^{10}		99.6		95.5	98
$*\frac{1^+}{2_1} \to \frac{1^-}{2_1}$	0.10×10^{10}				9.4	4
$\to \frac{3^-}{2_1}$	0.94×10^{9}				1.5	3
$\to \frac{3^+}{2_1}$	0.42×10^{9}	0.30×10^{10}			89.1	93
$\frac{7^+}{2_1} \to \frac{3^+}{2_1}$	0.36×10^{7}		<	<	<	<
$\to \frac{9^+}{2_1}$	0.96×10^{11}	0.65×10^{11}	100	100	100	100
$\frac{5^+}{2_1} \to \frac{1^+}{2_1}$	0.13×10^{9}		0.02	0.03	<	1
$\to \frac{3^+}{2_1}$	0.13×10^{12}	0.61×10^{11}	23.6	12.5	9.6	14
$\to \frac{7^+}{2_1}$	0.91×10^{9}	0.77×10^{10}	0.16	1.57	<	<
$\to \frac{9^+}{2_1}$	0.20×10^{12}		36.3	41	75	73
$\to \frac{3^-}{2_1}$	0.22×10^{12}		40	45	15.4	12
$\frac{11^+}{2_1} \to \frac{9^+}{2_1}$	0.36×10^{12}		100	100	99.3	100
$\to \frac{7^+}{2_1}$	0.29×10^{8}		0.01	0.01	0.07	<
$\frac{5^+}{2_2} \to \frac{9^+}{2_1}$	0.43×10^{12}		89.1	88.3	77.5	78
$\to \frac{5^+}{2_1}$	0.48×10^{9}	0.16×10^{11}	0.1	3.32	<	<
$\to \frac{1^+}{2_1}$	0.54×10^{9}		0.1	0.1	<	<
$\to \frac{3^+}{2_1}$	0.50×10^{11}	0.11×10^{11}	10.3	2.26	<	<
$\to \frac{7^+}{2_1}$	0.15×10^{10}	0.22×10^{11}	0.3	4.5	<	<
$\to \frac{3^-}{2_1}$	0.72×10^{10}		1.5	1.5	22.5	22
$\frac{11^+}{2_2} \to \frac{11^+}{2_1}$	0.34×10^{9}	0.58×10^{9}	0.7	1.08	<	<
$\to \frac{7^+}{2_1}$	0.41×10^{11}		88.7	76.5	91.1	100
$\to \frac{9^+}{2_1}$	0.49×10^{10}	0.12×10^{11}	10.6	22.4	8.9	<
$\frac{13^+}{2_1} \to \frac{11^+}{2_1}$	0.62×10^{10}	0.62×10^{11}	0.47	4.5	7.2	6
$\to \frac{11^+}{2_2}$	0.12×10^{9}	0.58×10^{8}	0.01	0.01	<	<
$\to \frac{9^+}{2_1}$	0.13×10^{13}		99.5	95.4	92.3	94
$\frac{9^+}{2_3} \to \frac{9^+}{2_1}$	0.30×10^{12}	0.80×10^{12}	53	57	(46.1)	22
$\to \frac{11^+}{2_1}$	0.30×10^{11}	0.16×10^{12}	5.3	11.4	(34.2)	<

TABLE II. (*Continued*)

$J^\pi \to J^\pi$	$P_{tot}(s^{-1})$ $g_R=Z/A$	$g_R=0$	Branching ratio $g_R=Z/A$	$g_R=0$	exp[a]	exp[b]
$\to \frac{11^+}{2_2}$	0.30×10^{10}	0.20×10^{11}	0.5	1.42	<	<
$\to \frac{7^+}{2_1}$	0.21×10^{12}	0.42×10^{12}	37.1	30	(19.7)	28
$\to \frac{7^+}{2_2}$	0.27×10^{8}	0.30×10^{9}	0.01	0.02	<	<
$\to \frac{5^+}{2_1}$	0.34×10^{10}		0.6	0.24	<	50
$\to \frac{5^+}{2_2}$	0.19×10^{9}		3.36	0.01	<	<
$\frac{7^+}{2_2} \to \frac{11^+}{2_1}$	0.29×10^{9}		0.01	0.01		34.2
$\to \frac{11^+}{2_2}$	<	<	<	<		<
$\to \frac{7^+}{2_1}$	0.44×10^{9}	0.11×10^{11}	0.02	0.1		19.7
$\to \frac{5^+}{2_1}$	0.20×10^{11}	0.29×10^{12}	1	2.5		<
$\to \frac{5^+}{2_2}$	0.52×10^{11}	0.47×10^{12}	2.5	4.02		<
$\to \frac{3^+}{2_1}$	0.74×10^{9}		0.4	0.01		<
$\to \frac{9^+}{2_1}$	0.20×10^{13}	0.11×10^{4}	96.4	93.4		46.1
$\frac{9^+}{2_2} \to \frac{9^+}{2_1}$	0.19×10^{13}	0.25×10^{13}	89.3	64.7	68.8	100
$\to \frac{11^+}{2_2}$	0.60×10^{9}	0.23×10^{11}	0.03	0.6	<	<
$\to \frac{11^+}{2_1}$	0.78×10^{11}	0.10×10^{13}	3.7	25.8	31.2(tentative)	
$\to \frac{9^+}{2_3}$	0.11×10^{10}	0.42×10^{10}	0.05	0.1	<	<
$\to \frac{7^+}{2_2}$	0.21×10^{10}	0.37×10^{11}	0.1	0.95	<	<
$\to \frac{7^+}{2_1}$	0.58×10^{12}	0.30×10^{12}	6.8	7.8	<	<

[a]Reference 7. [b]Reference 8.

tested in the foregoing discussion. We compare our calculations extensively with the experimental data of McDonald *et al.*[8] and Ø. Scheidemann *et al.*[7] in Table II.

The electromagnetic operators used for these calculations have been discussed in I; therefore we quote only the operators

$$M(E\lambda,\mu)=B(E\lambda;\lambda\to0)_{\rm Sn}^{1/2}[b_{\lambda\mu}^{+}+(-1)^{\mu}b_{\lambda-\mu}]$$
$$+\sum_{\alpha\beta}e_a\langle\alpha|r^{\lambda}Y_{\lambda\mu}|\beta\rangle C_{\alpha}^{+}C_{\beta} \qquad (3.2)$$

and

$$M(M1,\mu)=g_R R_{\mu}$$
$$+\sum_{\alpha\beta}\langle\alpha|g_l l_{\mu}+g_s s_{\mu}|\beta\rangle C_{\alpha}^{+}C_{\beta}. \qquad (3.3)$$

An effective proton charge $e_p^{\rm eff}=1.5e$ was used and gyromagnetic ratios $g_s=0.7g_s^{\rm free}$ and both $g_R=Z/A, 0$ have been considered. The value $g_R=0$ was shown to give in many cases the better agreement with experiment.[15,16] Pointing out some of the most important findings one obtains the following:

(i) For the highly retarded $E1$ transition rates, although the absolute rates are still off with some orders of magnitude,[8] the relative $E1$ rates do

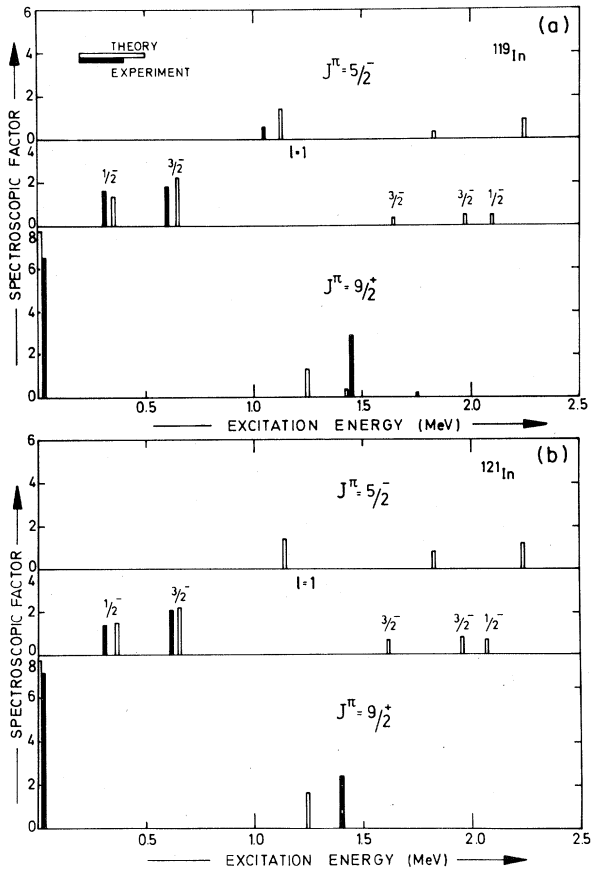

FIG. 3. (a) The spectroscopic factors for pickup, calculated with the unified-model wave functions and compared with the experimental data for ^{119}In of Weiffenbach. Both $l=4$, $l=3$, and $l=1$ transfer data are given. (b) Same as (a) but for ^{121}In.

resemble the experimental values rather well. (See Table II.)

(ii) For the vibrational multiplet members $J_i^\pi = \frac{11}{2}_1^+, \frac{5}{2}_2^+, \frac{13}{2}_1^+, \frac{9}{2}_2^+$, the decay pattern is well described by the unified-model wave functions, supporting—though model dependent—the assignment of the $|1g_{9/2}^{-1}, \mathrm{Sn}(2_1^+); \frac{9}{2}^+\rangle$ to the experimental $J^\pi = \frac{9}{2}^+$ level at 1.436 MeV.

(iii) For the $J_i^\pi = \frac{7}{2}_2^+$ and $\frac{9}{2}_3^+$ theoretical levels, the agreement with the 1.3885 MeV level $(\frac{7}{2}^+, \frac{9}{2}^+)$ does not seem to give a unique correspondence, although, on theoretical grounds, the $J_i^\pi = \frac{9}{2}_3^+$ assignment is more reasonable. Such a level was not observed by McDonald *et al.*[8]

(iv) A problem still remains for the experimental 1.353 MeV level with a $\frac{7}{2}^+, \frac{9}{2}^+$ assignment.[8] The decay pattern is definitely in contradiction with the $J_i^\pi = \frac{7}{2}_2^+$ assignment allowing the possibility for an explanation as the theoretical $J_i^\pi = \frac{9}{2}_4^+$ level, also as mainly a 1p-2h core coupled state.

(v) Then we conclude that the vibrational $|1g_{9/2}^{-1}, \mathrm{Sn}(2_1^+); \frac{7}{2}^+\rangle$ member has not been observed in ^{119}In.

(vi) For the other members of the rotational band, i.e., $J_i^\pi = \frac{7}{2}_1^+$ and $\frac{5}{2}_1^+$, the agreement between theory and experiment is satisfactory.

A general observation is the somewhat better agreement using the gyromagnetic ratio $g_R = 0$, when comparing with the experimental branching ratios. An analogous observation was already made by Paar.[15,16]

3. *Half-life of the $J_i^\pi = \frac{1}{2}_1^+$ level*

Here we have studied in some detail the highly collective $E2$ and retarded $M1$ transitions. Because, experimentally, the separate $E2$ and $M1$ partial half-lives were determined,[8] we can compare the results with the unified-model description in some detail (see Table III). The $E2$ contribution is reproduced very well with a theoretical result of $B(E2; \frac{1}{2}_1^+ \rightarrow \frac{3}{2}_1^+) = 0.374\ e^2\mathrm{b}^2$ (exp. $0.42^{+0.03}_{-0.17}\ e^2\mathrm{b}^2$).[8] This very fast $E2$ transition is mainly caused by the

$$|1g_{7/2},\ \mathrm{Cd}(4_1^+); \tfrac{1}{2}^+\rangle \rightarrow |1g_{7/2},\ \mathrm{Cd}(2_1^+); \tfrac{3}{2}^+\rangle$$

transition, being of the order of the $4_1^+ \rightarrow 2_1^+$ $E2$ transition in ^{118}Cd.

For the $M1$ part, a large dependence on g_R is observed, but even with $g_R = Z/A$, the $M1$ transition is not retarded enough. Taking into account the theoretical $E2$ and $M1$ conversion coefficients,[17] a total half-life $T_{1/2}(\mathrm{level}) = 1.24$ nsec (0.17 nsec) results for $g_R = Z/A, 0$ respectively, to be compared with the experimental value of 2.0 ± 0.2 nsec.

TABLE III. The $J_i^\pi \rightarrow \frac{1}{2}_1^+$ to $J_f^\pi = \frac{3}{2}_1^+$ gamma half-lives for both $g_R = Z/A$ and $g_R = 0$ (unified-model calculation). Comparison with the measurements of McDonald is given.

		$T_{1/2}(\gamma)$(s)			F
$J_i^\pi \rightarrow J_f^\pi$	Multipolarity	$g_R = Z/A$	$g_R = 0$	exp	exp
$\frac{1}{2}^+ \rightarrow \frac{3}{2}^+$	$M1$	3.0×10^{-9}	0.22×10^{-9}	$>7.9\times10^{-9}$	>850
$\frac{1}{2}^+ \rightarrow \frac{3}{2}^+$	$E2$	3.5×10^{-9}		3.1×10^{-9}	$\frac{1}{118}$

4. E2/M1 mixing ratio for the $J_i^\pi = \frac{3}{2}_1^-$ to $J_f^\pi = \frac{1}{2}_1^-$ transition

As the quantity $\delta(E2/M1)$ for the $\frac{3}{2}_1^- \to \frac{1}{2}_1^-$ has been measured for ^{117}In (Ref. 2) as -0.10 ± 0.02 or -1.40 ± 0.04 and in ^{119}In (Ref. 6) as -0.07 ± 0.02, we have calculated this quantity within the unified-model description. This will serve as a test of the collective components in both the $J_i^\pi = \frac{3}{2}_1^-$ and $J_f^\pi = \frac{1}{2}_1^-$ levels. In Figs. 4(a) and (b) we also give the dependence on the spin gyromagnetic ratio $g_s^{\rm eff}$ for both $g_R = Z/A$ and 0. The latter dependence appears to be small, but the g_s dependence is very pronounced. It appears that the value of g_s ($= 0.7 g_s^{\rm free}$) chosen for carrying out the calculation of magnetic properties reproduces rather well this particular mixing ratio.

Here, one again observes the importance of the collective admixtures in both the $J_i^\pi = \frac{3}{2}_1^-$ and $J_f^\pi = \frac{1}{2}_1^-$ levels which we give as an example, i.e.,

$$\left|\tfrac{1}{2}_1^-\right\rangle = 0.86\left|2p_{1/2}\right\rangle + 0.35\left|2p_{3/2}, \mathrm{Sn}(2_1^+); \tfrac{1}{2}^-\right\rangle - 0.30\left|1f_{5/2}, \mathrm{Sn}(2_1^+); \tfrac{3}{2}^-\right\rangle ,$$

$$\left|\tfrac{3}{2}_1^-\right\rangle = 0.74\left|2p_{3/2}\right\rangle - 0.42\left|2p_{1/2}, \mathrm{Sn}(2_1^+); \tfrac{3}{2}^-\right\rangle + 0.29\left|2p_{3/2}, \mathrm{Sn}(2_1^+); \tfrac{3}{2}^-\right\rangle .$$

If one completely excludes these collective admixtures, the $B(E2)$ value is reduced by an order of magnitude, thus giving an idea of the influence of collective $E2$ components.

5. Vibrational yrast structure

Because we consider a harmonic underlying Sn quadrupole vibrational structure, the yrast sequence of $J_i^\pi = \frac{9}{2}_1^+, \frac{11}{2}_1^+, \frac{13}{2}_1^+, \frac{15}{2}_1^+, \frac{17}{2}_1^+$ can be easily identified, at least for the lowest three members in ^{119}In, due to the observed γ deexcitation pattern from the excited states decaying preferentially with $E2$ transitions. Sometimes, as is the case in ^{119,121}In, other states with similar J^π values can occur at the relevant excitation energy and mask a simple observation of the yrast vibrational multiplet states. Therefore, electromagnetic properties are of much interest and, moreover, show a strong dependence on the nature (vibrational, rotational) of the levels. A similar analysis has been made for ^{109}In (Ref. 19) and for ^{111}In (Ref. 20), where experimental δ values and $B(E2)$ crossover to cascade ratios were determined. The following expressions result for the mixing ratio δ, in lowest order perturbation theory for, respectively, yrast transitions inside the multiplet ($\Delta N = 0$) and for transitions between different multiplet members ($\Delta N = 1$), i.e.,

$$\frac{\langle\|E2\|\rangle}{\langle\|M1\|\rangle} = \frac{\sqrt{5}}{2j}\left(\frac{j+2N+1}{j+2N-2}\right)^{1/2} \frac{Q(j)}{g_j - g_R} \quad (\Delta N = 0) \tag{3.4}$$

and

$$\frac{\langle\|E2\|\rangle}{\langle\|M1\|\rangle} = \frac{16\sqrt{5\pi}\, j(j+1)[NB(E2; 2 \to 0)]^{1/2}}{3(2j-1)[5N(j+2N-2)(j+2N)]^{1/2}} \times \frac{1}{\xi} \frac{Q(j)}{(g_j - g_R)|Q(j)|} \quad (\Delta N = 1). \tag{3.5}$$

For the $B(E2)$ crossover to cascade ratios two distinct groups occur:

(i) branching of a $\Delta N = 1$ and a $\Delta N = 0$ transition, both from the highest spin member of a multiplet

$$\frac{B(E2; \Delta N = 1)}{B(E2; \Delta N = 0)} = \frac{8\pi j(j+2N)(j+2N-1)}{15N(j+2N+1)} \times \frac{B(E2; 2 \to 0)N}{Q(j)^2}, \tag{3.6}$$

and

(ii) branching of two $\Delta N = 1$ transitions, connecting levels with $J_i = J_{\max} - 1$ of the N phonon multiplet with the two highest spin states of the $N-1$ phonon multiplet

$$\frac{B(E2; \Delta N = 1; \Delta J = 2)}{B(E2; \Delta N = 1; \Delta J = 1)} = \frac{(N-1)(j+2N)}{j}. \tag{3.7}$$

In each formula, N gives the number of phonons in the initial state, $Q(j)$ the quadrupole moment of the single-hole configuration, and ξ the hole-core coupling strength.

In ^{119,121}In, no experimental numbers for the quantities (3.4)–(3.7) are determined. We calculate, however, (see Figs. 5 and 6) the expected behavior of, respectively, δ and $B(E2)$ ratios from the unified-model description (diagonalization) as well as from a perturbation theory analy-

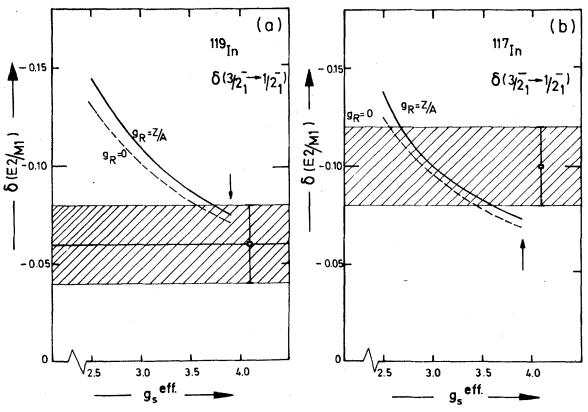

FIG. 4. (a) The $\delta(E2/M1)$ mixing ratio as calculated for ^{119}In. Both results for $g_R = Z/A$ and $g_R = 0$ are drawn as a function of the spin gyromagnetic ratio g_s. The experimental value with error bar is drawn. The small arrow indicates the $g_s^{\rm eff}$ value used in all the $M1$ calculations. (b) Same as (a) but for ^{117}In.

sis. In making the lowest order perturbation theory calculation, the $B(E2; 2_1^+ \rightarrow 0_1^+)$ value of ^{120}Sn (0.0412 e^2b^2) was considered.[5] Since the $J_i^\pi = \frac{9}{2}_1^+$ quadrupole moment for ^{119}In is unknown, we took for $Q\ (1g_{9/2}^{-1})$ the experimental value as determined for ^{115}In, i.e., $Q\ (\frac{9}{2}_1^+) = 0.83$ eb.[21] In order to compare with the analogous quantities in a deformed description, i.e., supposing the sequence $\frac{9}{2}_1^+, \frac{11}{2}_1^+, \frac{13}{2}_1^+, \frac{15}{2}_1^+, \frac{17}{2}_1^+, \ldots$ would form a rotational band on a $\frac{9}{2}^+$ band head, we considered the rotational quantities for the mixing ratio δ,

$$\frac{\langle \|E2\| \rangle}{\langle \|M1\| \rangle} = \sqrt{5}\,\frac{Q_0(\Omega)}{g_\Omega - g_R}\left[\frac{1}{(2J_i+1)(2J_i-1)}\right]^{1/2}, \tag{3.8}$$

and for the $B(E2)$ crossover to cascade ratio,

$$\frac{B(E2;\Delta J=2)}{B(E2;\Delta J=1)} = \frac{(J_i-1+\Omega)(J_i-1-\Omega)}{2\Omega^2} \times\left(\frac{J_i+1}{2J_i-1}\right). \tag{3.9}$$

Knowing that for a pure band $g_\Omega = g_j$, we determined for ^{119}In $Q_0(\frac{9}{2}^+) = 1.52$ eb [related to $Q\ (1g_{9/2}^{-1})$ = 0.83 eb through the laboratory to intrinsic frame transformation], we also show the results of Eqs. (3.8) and (3.9) in Figs. 5 and 6. The latter expressions give rise to a very smooth behavior of δ and $B(E2)$ ratios on the angular momentum whereas in the vibrational description, the oscillatory behavior of both δ and $B(E2)$ ratios becomes very pronounced. It can, moreover, be pointed out that the sign of the mixing ratio δ $(E2/M1)$ in the vibrational model, given by $Q(j)/(g_j - g_R)$, is closely related to the value in the rotational model, given by $Q_0(\Omega)/(g_\Omega - g_R)$ (Ref. 22). In the light of the very pronounced dependence on angular momentum for the yrast levels, measurements for the quantities as discussed above are of much interest.

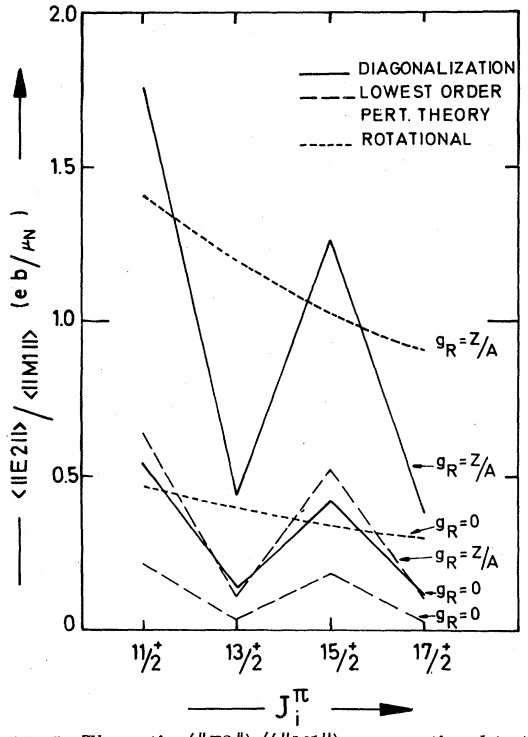

FIG. 5. The ratio $\langle \|E2\| \rangle / \langle \|M1\| \rangle$, proportional to the mixing ratio $\delta(E2/M1)$, for both the full diagonalization and the lowest order perturbation theory, as well as the rotational limit, in ^{119}In. Calculations with $g_R = Z/A$ and $g_R = 0$ have been carried out. Only the initial spin J_i^π is drawn on the horizontal axis.

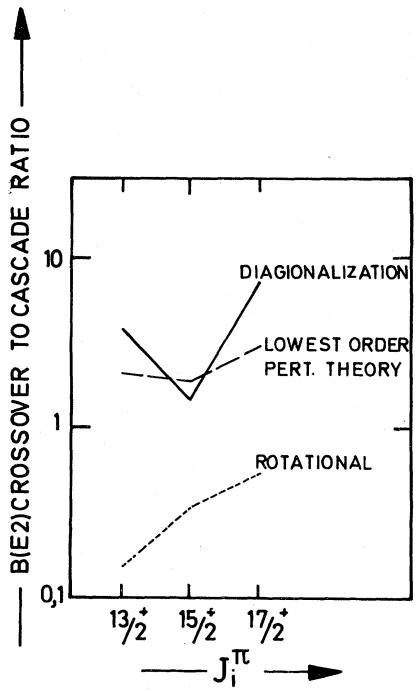

FIG. 6. The $B(E2)$ crossover to cascade ratio for ^{119}In. Only the initial state angular momentum J_i^π is indicated on the horizontal axis. Results from both the full diagonalization and the perturbation theory in lowest order, as well as the rotational limit, are given.

IV. DEFORMED CALCULATIONS

The origin of the low-lying positive-parity "intruder" states has been already suggested to be the $\frac{1}{2}^+$ [431] Nilsson orbital.[23,24] Recently, more detailed calculations on the total potential energy (TPE) surfaces for odd-mass In were carried out,[25] clearly indicating a pronounced minimum associated with the $\frac{1}{2}^+$ [431] Nilsson orbital. Carrying out these calculations from ^{107}In to ^{121}In, the excitation energy as a function of the quadrupole deformation ϵ_2 at the deformed

minimum is given in Fig. 7. The way excitation energy is defined is discussed in detail in Ref. 26. The parameters of the Nilsson model ($\kappa_{p,n}$; $\mu_{p,n}$ and $G_{p,n}$ the pairing strength) are the same as used in calculations of Ragnarsson.[25]

Simple $\frac{1}{2}^+$ [431] pure rotational band fits, however,[8,25] do not yield very good agreement and, moreover, need especially large decoupling coefficients[8] $a = -2.0$ to -4.0 (in going from ^{115}In to ^{119}In), compared with the decoupling parameters as calculated from the $\frac{1}{2}^+$ [431] Nilsson orbital, being an order of magnitude smaller on the average.

A. Band-mixing calculations

We have performed a complete band-mixing calculation for ^{119,121}In. Therefore, we took into account all Nilsson orbitals originating from the $N=4$ harmonic oscillator shell and performed the band mixing at the equilibrium deformation of the $\frac{1}{2}^+$ [431] orbital. Strong mixing with the nearby $\frac{1}{2}^+$ [420] and $\frac{3}{2}^+$ [422] orbitals occurs, and modifies the rotational-band structure considerably. Moreover, this calculation serves as an explanation for the otherwise unreasonably large decoupling coefficient a used in the pure $\frac{1}{2}^+$ rotational-band fits of Ref. 8.

Without going into detail, in the formalism (energy matrix elements, different representations, electromagnetic operators, and electromagnetic matrix elements; see Refs. 1 and 27), the resulting energy spectra for ^{119,121}In are shown in Fig. 8, where the levels of deformed

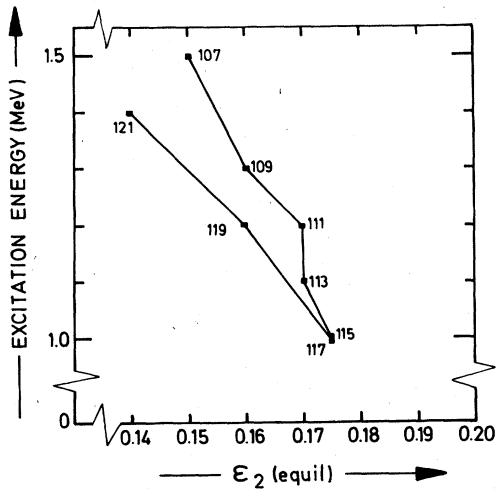

FIG. 7. The excitation energy E_x as a function of the equilibrium deformation ϵ_2 for the $\frac{1}{2}^+$ [431] Nilsson orbital. Results of total potential energy surfaces for this orbital, for all odd-mass In nuclei are summarized.

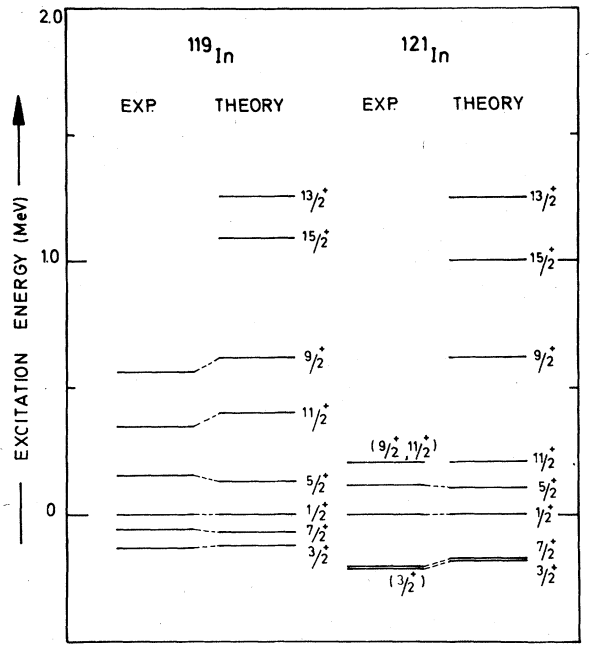

FIG. 8. Resulting energy spectra from band-mixing calculations (full $N=4$ harmonic oscillator shell), compared with the experimental data, for positive-parity, rotational-like levels in ^{119,121}In. Calculations are normalized to the energy position for the lowest $J^\pi = \frac{1}{2}^+$ level.

nature are drawn relative to the $J^\pi = \frac{1}{2}^+$ band head level. A very good agreement occurs in ^{119}In, and even for ^{121}In where some of the spin assignments are still tentative.[6,7] In order to obtain such an agreement, we had to vary μ_p (Nilsson model parameter) from 0.525 to 0.550 in going from ^{119}In to ^{121}In. This change reflects the relative variation in single-particle energy of the $2d_{5/2}$ proton level with respect to the $1g_{7/2}$ proton level as observed in the odd-mass Sb isotopes also.[28-30] This change of a macroscopic parameter of the Nilsson model (μ_p) is necessary to describe local changes in the single-particle ordering, which, on the microscopic level, should be due to short-range proton-neutron interactions when changing the number of neutrons.[28-30]

B. Electromagnetic properties

With the wave functions obtained in Sec. IV A, spectroscopic factors for stripping into levels above $Z=50$ as well as electromagnetic properties (moments and transition rates) can easily be calculated. Since detailed expressions have been discussed at some length,[27] only the results will be discussed.

In Fig. 9 we show the quadrupole moments for

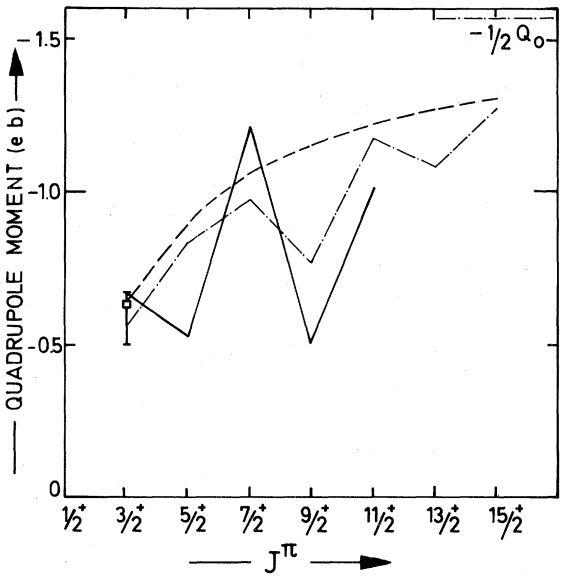

FIG. 9. The quadrupole moment of the rotational-like states in ^{119}In, as calculated in the deformed representation for band mixing (dashed-dot line) and a pure $\frac{1}{2}^+$ [431] band (dashed line). The results of the unified-model calculations are also drawn (full line). The rotational limit ($-\frac{1}{2}Q_0$) is also indicated.

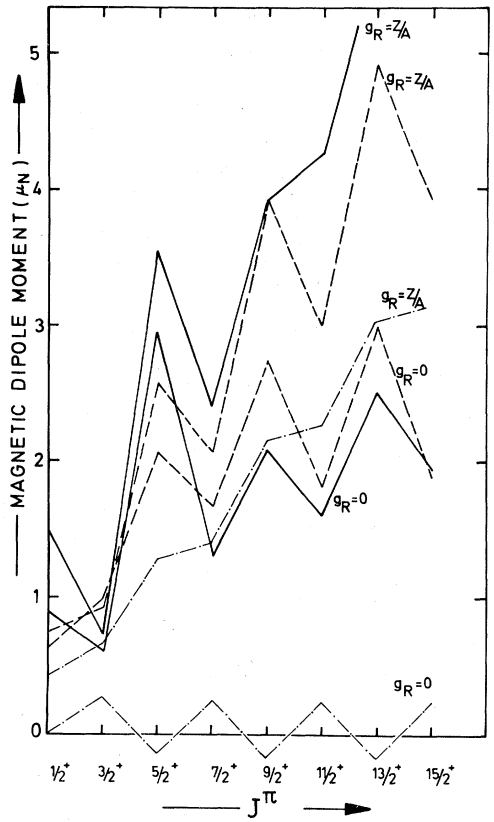

FIG. 10. Magnetic dipole moments for the rotational-like states in ^{119}In as calculated in the deformed representation [band mixing (dashed line) and a pure $\frac{1}{2}^+$ [431] band (dashed-dot line)] for both $g_R = Z/A$ and $g_R = 0$. The analogous results from the unified-model calculations are given (full line). In all cases, the effective spin gyromagnetic ratio $g_s^{\text{eff}} = 0.7\, g_s^{\text{free}}$ was used.

the pure $\frac{1}{2}^+$ [431] band, for the complete band-mixing wave functions as well as for the unified model starting from a completely different zero-order description. For the $J^\pi = \frac{3}{2}^+$ level, we indicate as the experimental value a quadrupole moment as deduced from the rotational analysis of McDonald[8] (there Table 5, converted to the laboratory system). Also the rotational limit for the quadrupole moment (for $J \to \infty$; $Q \to -\frac{1}{2}Q_0$) is drawn in this figure.

In Fig. 10, the magnetic dipole moments for the pure $\frac{1}{2}^+$ [431] band are given for the mixed bands and for the unified-model calculations, both with the extreme values of g_R as Z/A and 0.

The general behavior is again similar in both descriptions. The general trend $\mu \cong g_R J$ of a deformed description is observed with a very pronounced saw-tooth structure because of the

$$(g_\Omega - g_R)\left(\frac{\Omega^2}{J(J+1)}\right)[1+(-1)^{J+1/2}(2J+1)b_0\delta_{\Omega,1/2}] \tag{4.1}$$

contribution.[31] For the pure $\frac{1}{2}^+$ [431] orbital, the macroscopic parameters (g_Ω, b_0) become (0.86, −0.85) and (0.86, −0.53) for, respectively, $g_s = 0.7\, g_s^{\text{free}}$ and $g_R = Z/A$, $g_R = 0$.

Finally, in Table IV, the $B(E2)$ and $B(M1)$ reduced transition probabilities for the deformed description are given, both for a pure $\frac{1}{2}^+$ [431] band as well as for the full band-mixing wave functions.

The $J_i^\pi = \frac{3}{2}^+ \to J_f^\pi = \frac{1}{2}^+$ $B(E2)$ value is known[8] ($= 21^{+2}_{-9}\, e^2b^2\, 10^{-2}$) and compares very well with the calculated values. From these results, very strikingly, the $\Delta J = 2$ and $\Delta J = 1$ intensity rules result. For the $B(M1)$ values, important differences occur between the pure and mixed wave functions, although again, strong alteration in the intensity results. This is due to the b_0 coefficient in the $B(M1)$ expression,[31] occuring with the phase factor

$$B(M1; J_i \to J_f) \simeq [1+(-1)^{J>+1/2}\delta_{\Omega,1/2}b_0]^2 . \tag{4.2}$$

V. CONCLUSION

We have shown that, taking into account the coupling of both 1h and 1p-2h (senority $v = 1$ and $v = 3$) configurations to the quadrupole and octu-

TABLE IV. Within the deformed description, as a result of band mixing, the $B(E2)$ and $B(M1)$ within the $\frac{1}{2}^+, \frac{3}{2}^+, \ldots$ rotational-like band sequence, The results for a pure $\frac{1}{2}^+[431]$ band are also given for comparison.

$J_i^\pi \to J_f^\pi$	$B(E2)\times 10^{-2} e^2b^2$ Pure	$B(E2)\times 10^{-2} e^2b^2$ Mixed	$B(M1)\times 10^{2}(\mu_N)^2$ Pure	$B(M1)\times 10^{2}(\mu_N)^2$ Mixed
$\frac{3}{2}^+ \to \frac{1}{2}^+$	20.0	14.7	0.0076	1.64
$\frac{5}{2}^+ \to \frac{1}{2}^+$	20.0	17.1		
$\to \frac{3}{2}^+$	5.7	4.6	1.41	0.32
$\frac{7}{2}^+ \to \frac{3}{2}^+$	25.7	22.5		
$\to \frac{5}{2}^+$	2.86	2.29	0.0098	0.34
$\frac{9}{2}^+ \to \frac{5}{2}^+$	28.6	21.7		
$\to \frac{7}{2}^+$	1.74	1.33	1.57	0.056
$\frac{11}{2}^+ \to \frac{7}{2}^+$	30.3	29.0		
$\to \frac{9}{2}^+$	1.16	0.88	0.01	0.0078
$\frac{13}{2}^+ \to \frac{9}{2}^+$	31.5	15.6		
$\to \frac{11}{2}^+$	0.84	0.71	1.63	3.21
$\frac{15}{2}^+ \to \frac{11}{2}^+$	32.3	31.5		
$\to \frac{13}{2}^+$	0.63	0.57	0.011	0.023

pole vibrations of the underlying core nucleus, a rich variety of nuclear phenomena results. Both the vibrational $|1g_{9/2}^{-1}, \mathrm{Sn}(2_1^+); J^\pi\rangle$ multiplet as well as the rotational-like sequence $J^\pi = \frac{1}{2}^+, \frac{3}{2}^+, \ldots$ are reproduced. Moreover, the unified-model wave functions describe rather well nuclear reaction (pickup) as well as electromagnetic transition properties [branching ratios, $T_{1/2}(\frac{1}{2}^+_1)$; the $\delta(E2/M1)$ mixing ratio for the $J_i^\pi = \frac{3}{2}^-_1$ to $J_f^\pi = \frac{1}{2}^-_1$ transition]. We further discuss for the yrast states from the vibrational multiplet, electromagnetic properties such as mixing ratios and $B(E2)$ ratios, calculated in lowest order perturbation theory and with the full unified-model wave functions. Comparison with a deformed description was also carried out.

Finally, and in order to understand better the equivalence between a rotational description and calculations as performed in our unified-model description, extensive band-mixing calculations have been carried out, taking all $N=4$ Nilsson orbitals. Furthermore, also electromagnetic properties within a deformed picture were calculated and compared to calculations starting from a spherical basis. In this way, a clear equivalence results concerning the $J^\pi = \frac{1}{2}^+$ rotational-like band between both description starting from opposite zero order Hamiltonians.

What now remains is to study the systematics of all odd-mass In isotopes ($A=107$ to $A=123$) and global features. This will be the content of a forthcoming article.

ACKNOWLEDGMENTS

The authors are indebted to Professor A. J. Deruytter for his interest during the course of this work. One of the authors (K.H.) is most grateful to Professor R. Chery, the IN2P3 for financial support, and discussions with Dr. J. Sau in the final stages of this work. We also wish to acknowledge beneficial discussions with Dr. R. A. Meyer, Dr. W. B. Walters, and Dr. W. Hesselink.

[1] K. Heyde, M. Waroquier, and R. A. Meyer, Phys. Rev. C 17, 1219 (1978).
[2] M. D. Glascock, E. W. Schneider, W. B. Walters, S. V. Jackson, and R. A. Meyer, Phys. Rev. C 20, 2370 (1979).
[3] Here, R is a shorthand notation for $(N_oR_o, N_qR_q)R$, where N and R denote the number of phonons and the angular momentum, respectively. The labels o and q mean octupole or quadrupole type of vibration.
[4] Here (I,i) denote the angular momentum and i an order number to separate different I states, i.e., $i=1,2,\ldots$.
[5] C. K. Ross and R. K. Badhuri, Nucl. Phys. A196, 369 (1976).
[6] S. Idzenga, Ph.D. thesis, VU Amsterdam, 1979 (unpublished).
[7] Ø. Scheidemann, E. Hagebø, P. Patzelt, and Isolde Collaboration CERN, J. Inorg, Nucl. Chem. 38, 1757 (1976).
[8] J. McDonald, B. Fogelberg, A. Bäcklin, and Y. Kawase, Nucl. Phys. A224, 13 (1974).
[9] C. V. Weiffenbach and R. Tickle, Phys. Rev. C 3, 1668 (1971).
[10] J. W. Smits and R. H. Siemssen, Nucl. Phys. 261, 385 (1976).
[11] A. H. Wapstra and K. Bos, At. Data Nucl. Data Tables 19, 17 (1977).
[12] B. S. Rehal and R. A. Sorensen, Phys. Rev. C 2, 819 (1970).
[13] W. B. Walters, private communication.
[14] S. Idzenga, private communication.
[15] V. Paar, Nucl. Phys. A211, 29 (1973).
[16] V. Paar, *Problems of Vibrational Nuclei*, edited by

G. Alaga, V. Paar, and L. Sips (North-Holland, Amsterdam, 1975), p. 15.
[17]R. S. Hager and E. C. Seltzer, Nucl. Data Tables A4, 1 (1968).
[18]M. D. Glascock, E. W. Schneider, P. W. Gallagher, W. H. Zoller, S. V. Jackson, W. B. Walters, and R. A. Meyer (unpublished).
[19]A. Van Poelgeest, Ph.D. thesis, VU Amsterdam, 1978 (unpublished); A. Van Poelgeest, W. H. A. Hesselink, J. Bron, J. J. A. Zalmstra, M. J. Uitzinger, H. Verheul, S. J. Feenstra, and J. Van Klinken, Nucl. Phys. A327, 12 (1979).
[20]W. H. A. Hesselink, J. Bron, P. M. A. Vander Kam, and V. Paar, Nucl. Phys. A299, 60 (1978).
[21]G. F. Fuller and V. W. Cohen, Nucl. Data Sect. B 9, Appendix 1 (1965).
[22]V. Paar, Phys. Lett. 80B, 20 (1978).
[23]A. Bäcklin, B. Fogelberg, and S. G. Malmskog, Nucl. Phys. A96, 539 (1967).
[24]R. A. Meyer, in *Problems of Vibrational Nuclei*, edited by G. Alaga, V. Paar, and L. Sips (North-Holland, Amsterdam, 1968).
[25]W. Dietrich, A. Bäcklin, C. O. Lannergard, and I. Ragnarsson, Nucl. Phys. A253, 429 (1975).
[26]K. Heyde, M. Waroquier, P. Van Isacker, and H. Vincx, Phys. Lett. 64B, 135 (1976).
[27]K. Heyde, M. Waroquier, P. Van Isacker, and H. Vincx, Nucl. Phys. A292, 237 (1977).
[28]L. Silverberg, Ark. Fys. 20, 341 (1961).
[29]E. Baranger, in *Advances in Nuclear Physics*, edited by M. Baranger and E. Vogt (Plenum, New York, 1971), Vol. 4, p. 261.
[30]G. Vanden Berghe and K. Heyde, Nucl. Phys. A167, 478 (1971).
[31]A. Bohr and B. R. Mottelson, *Nuclear Structure* (Benjamin, New York, 1969 and 1975), Vols. 1 and 2.